Topological Aspect and Quantum Magnetoresistance of β-Ag_2Te

Wei Zhang, Rui Yu, Wanxiang Feng, Yugui Yao, Hongming Weng,* Xi Dai,† and Zhong Fang‡

Beijing National Laboratory for Condensed Matter Physics, and Institute of Physics, Chinese Academy of Sciences, Beijing 100190, China

(Received 6 January 2011; revised manuscript received 17 February 2011; published 14 April 2011)

To explain the unusual nonsaturating linear magnetoresistance observed in silver chalcogenides, the quantum scenario has been proposed based on the assumption of gapless linear energy spectrum. Here we show, by first principles calculations, that β-Ag_2Te with distorted antifluorite structure is in fact a topological insulator with gapless Dirac-type surface states. The characteristic feature of this new binary topological insulator is the highly anisotropic Dirac cone, in contrast with known examples, such as Bi_2Te_3 and Bi_2Se_3. The Fermi velocity varies an order of magnitude by rotating the crystal axis.

DOI: 10.1103/PhysRevLett.106.156808 PACS numbers: 72.25.Ba, 71.20.−b, 73.20.−r

Ag_2Te, one of silver chalcogenides, is known as Hessite mineral in nature. It was used as ionic conductor at high temperature α phase, and it undergoes a phase transition below 417 K into the β phase, a narrow gap semiconductor, where the ion migration is frozen and the compound is nonmagnetic. The gap of β-Ag_2Te is in the range of several tens meV [1], the mobility of carriers is high and the effective mass is of the order of $10^{-2}m_0$ (m_0 is the free electron mass) [2]. Unusually large and nonsaturating linear magnetoresistance (MR) were observed in β-$Ag_{2+\delta}Te$ for the field range 10–55000 Oe and temperature range 4.5–300 K [3], in contrast to the conventional theory of metal with closed Fermi surface, from which the quadratic (low-field) and saturating (high-field) MR is expected. This leads to the proposal of quantum MR by Abrikosov [4], where only the lowest Landau level remains occupied. However, for a quadratic energy spectrum, the Landau level spacing (which depends on the field linearly) is about 0.1 K estimated for β-Ag_2Te at 10 Oe), which is too small [4]. It is therefore necessary to assume the gapless linear energy spectrum [4], such that the field dependence of Landau level spacing follows the square root rule ($\Delta E_n \propto \sqrt{B}$), similar to case of graphene. The linear energy spectrum may come from the strong disorder as pursued by Abrikosov; however, we will show in this Letter that β-Ag_2Te is in fact a topological insulator with gapless linear Dirac-type surface states. This raises the possibility that the observed unusual MR may largely come from the surface or interface contributions.

Topological insulator (TI), characterized by the Z_2-invariance and protected by the time-reversal symmetry, is a new state of quantum matter [5–9]. It is different from trivial insulator in the sense that its bulk is insulating, while its surface supports metallic Dirac fermions. Exotic quantum phenomena, such as Majorana fermion [10], magnetoelectric effect [11], and quantum anomalous Hall effect [12], are expected from TIs. TI can be realized in 2D systems, such as HgTe/CdTe quantum well [13], or 3D materials like $Bi_{1-x}Sb_x$ [14]. The discovery of Bi_2Se_3 family TIs with single Dirac cone on the surface is a significant progress [15], where the bulk gap is as large as 0.3 eV, which makes the room temperature applications possible. There are several more recent proposals, such as $TlBiX_2$ (X = Te, Se) compounds [16], ternary Heusler alloys [17], chalcopyrites [18], which all involve three or more elements, and may require additional distortions to open up the bulk gap. For all known TIs up to now, the surface Dirac cones are almost isotropic and Fermi velocity is nearly a constant. Here we will show that highly anisotropic surface Dirac cone can be obtained in β-Ag_2Te, a new binary TI with distorted antifluorite structure.

We calculate the electronic structures of Ag_2Te by using the WIEN2K package. The generalized gradient approximation (GGA) is used for the exchange-correlation functional, and Brillouin zone (BZ) is sampled with $21 \times 21 \times 21$ grids for α phase and $10 \times 10 \times 10$ for β phase. We construct the projected atomic Wannier (PAW) functions [19] for s and p orbitals of Ag and Te. With this set of PAW bases, an effective model Hamiltonian for a slab of 45 layers along the C axis is established and the topologically nontrivial surface state is obtained from it [20].

The high temperature α phase of Ag_2Te can be regarded as the antifluorite structure (Fig. 1) in average [21]. Defining the cubic translational vectors as a, b, c, this structure can be constructed from three fcc sublattices called as Te, Ag(1) and Ag(2) sublattice, respectively. The Ag(1) sublattice is shifted from the Te one by a vector ($a/4$, $b/4$, $c/4$). If we only consider the Te and Ag(1) sublattices, it gives the same structure as zinc blende (like HgTe or CdTe). Adding the additional Ag(2) sublattice, which is shifted from original Te-fcc one by ($-a/4$, $-b/4$, $-c/4$), the antifluorite structure is obtained. Without distortions, the Ag(1) and Ag(2) sublattices are equivalent, and the space group is Fm3m with the inversion symmetry included. From the other point of view, if we divide the large cube defined by a, b, c into 8 small cubes, only 4 out of 8 cube's body centers are occupied in zinc blende, but they are now all occupied in antifluorite. All Ag

 © 2011 American Physical Society

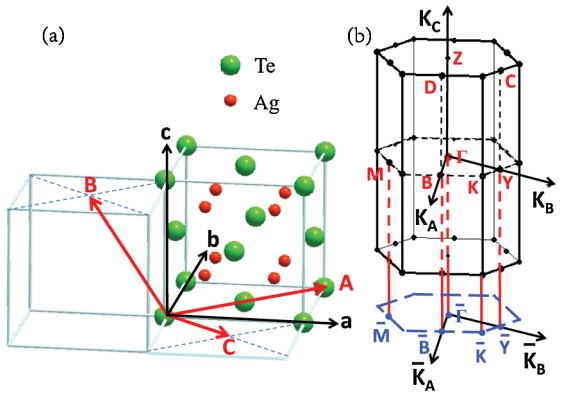

FIG. 1 (color online). (a) The cubic antifluorite structure of α-Ag_2Te and its structural relationship to the β phase. The translational vectors of α and β phases are labeled as a, b, c and A, B, C, respectively. (b) The Brillouin zone of β-Ag_2Te, and its projected surface BZ to the plane perpendicular to C axis.

atoms in α-Ag_2Te are tetrahedrally coordinated by four nearest neighboring Te atoms.

Figure 2 shows the calculated band structure and density of states of α-Ag_2Te (with optimized lattice parameter $a = 6.8$ Å). The electronic structure can be well understood as zero-gap semiconductor, similar to HgTe, with inverted band ordering around the Γ point. In conventional zinc blende semiconductor, the anion-p states (Te-5p) at Γ point split into Γ_8 and Γ_7 manifolds due to the spin-orbit coupling (SOC) with Γ_8 forming the valence band maximum (VBM). The conduction band minimum (CBM) is mostly from the cation-s state, called as Γ_6. The Γ_6 is typically higher than the Γ_8 and Γ_7, such as in CdTe, and a positive gap is formed. For HgTe, however, the situation is different due to the presence of Hg-5d states, which are

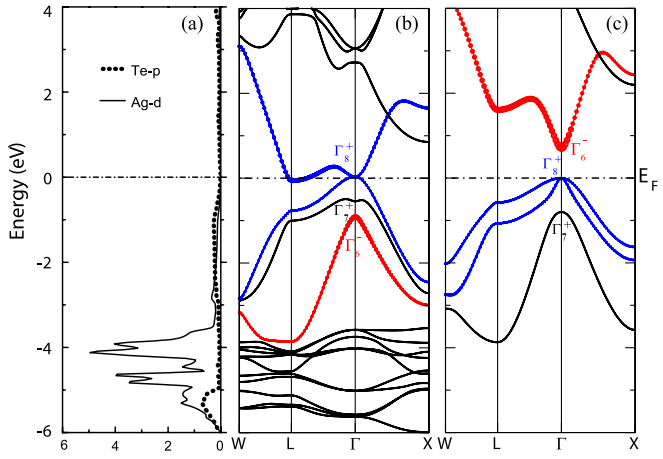

FIG. 2 (color online). The calculated electronic structure of α-Ag_2Te. (a) The projected density of states for Te-p and Ag-d states, respectively. (b) The original band structure and (c) the one after pushing Ag-4d states artificially down to -20 eV. The projected component of Ag s orbital is indicated as fat bands, and the characters of low-energy wave functions around the Γ point are indicated as $\Gamma_6, \Gamma_7, \Gamma_8$. Colors are used to guide the eyes.

very shallow and hybridize with Te-5p states strongly. Such hybridization will push the Te-5p upwards, resulting in an inverted band structure with the Γ_6 state lower than the Γ_8 (therefore a negative band gap). Because of the fourfold degeneracy of Γ_8 manifolds, the zero-gap semiconductor is formed. The antifluorite structure of α-Ag_2Te is similar to zinc-blende, and its band structure is also very similar to HgTe. The Te sites form the same fcc sublattice with similar lattice parameters ($a = 6.8$ Å for Ag_2Te and $a = 6.46$ Å for HgTe), but with two Ag atoms instead of single Hg atom in the unit cell. The low-energy states of α-Ag_2Te can be also characterized as Γ_6, Γ_7, Γ_8. The Ag-4d level is again very shallow, located mostly from -6.0 eV to -3.5 eV as shown in Fig. 2. Since the Ag-4d orbitals are less extended than the Hg-5d orbitals, less p-d hybridization may be expected. However, because there are two Ag sites (instead of one Hg atom in HgTe) in one unit cell, the p-d hybridizations are strong enough to push up the Te-5p states and leads to the inverted band structure [Fig. 2(b)] with Γ_6 lower than Γ_8. To further demonstrate this mechanism, we have shown in Fig. 2(c) the calculated band structure of α-Ag_2Te by artificially pushing the Ag-4d states down to -20 eV (out of the figure). Because of the reduced p-d hybridization, the Te-4p states are now lower than the Ag-5s states, giving a positive band gap.

The above calculations were done based on the GGA, which is known to underestimate the band gap of semiconductors (charge-transfer gap). The situation now is different from Bi_2Te_3 and Bi_2Se_3, where the gap is formed within the p manifolds, and mostly due to the SOC, which is a local physics and can be well described by the GGA (or LDA) [15]. The band gap problem for HgTe and HgSe has been carefully studied by GW calculations and semiempirical method [22], as well as comparing with experiments. It has been quantitatively suggested that the LDA underestimates the band gap of HgTe (or HgSe) by the magnitude around 0.3–0.6 eV [22]. Considering the strong similarity between α-Ag_2Te and HgTe as discussed above, the same size of the error bar from LDA (or GGA) may be expected. Nevertheless, even if the 0.6 eV correction for the band gap is added, the resulting band structure still supports the inverted band ordering at Γ. This is because the calculated Γ_6 in GGA is far below the Γ_8 (about -1.0 eV), a number much bigger than the possible error bar for those compounds. This result is further confirmed by our calculations using hybrid functional [23]. As long as the inverted band ordering remains for Ag_2Te, the topological nature can be expected as discussed for HgTe [13].

To turn a cubic zero-gap compound into a true semiconductor, certain distortion or strain has to be introduced to break the degeneracy of Γ_8 manifolds. This strategy has been followed for some of predicted topological insulators, such as Heusler alloys [17], although artificial distortions are not always easy. In our case, however, the Ag_2Te

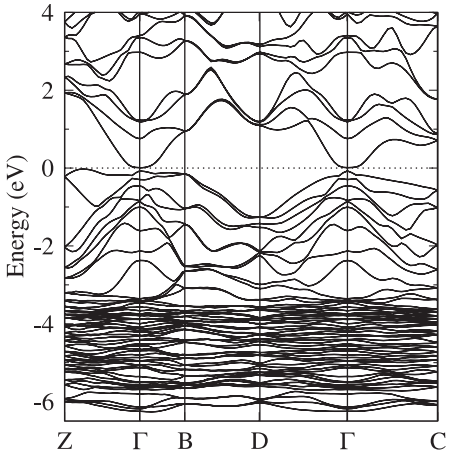

FIG. 3. The calculated electronic structure of β-Ag_2Te including spin-orbit coupling. A gap is opened around the Fermi level (dotted line).

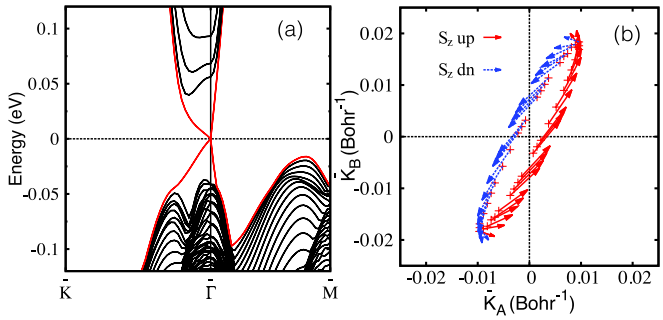

FIG. 4 (color online). The surface states of β-Ag_2Te for the surface perpendicular to the C axis. (a) The surface band structure and Dirac cone calculated from a slab of 45 layers; (b) The Fermi surface and spin texture of surface states with chemical potential located 10 meV below Dirac point. The in-plane compents of spin are indicated as arrows, while the red (blue) color means the out-of-plane components pointing out-(in-) ward of the plane. The penetration depth of the surface states is about 3 nm.

undergoes structural distortion in its natural way: the high temperature α phase changes into the β phase below 417 K, and the crystal structure of β-Ag_2Te can be understood as the distorted antifluorite structure as shown in Fig. 1. Starting from the cubic α phase with translational vectors a, b, c, we can define three new translational vectors $A = a + b$, $B = -a/2 - b/2 + c$, $C = a/2 - b/2$. Then the distortion happens in such a way that both the lengths of A, B, and C vectors and the angle between the A and B axis are varied, while keeping the C axis perpendicular to the AB plane. The atomic positions are also shifted from their high-symmetrical position, resulting in the monoclinic structure with space group $P2_1/c$ [24]. Although the distortions are a bit complicated, the main effect of distortions is to open up a gap around the Fermi level. Figure 3 shows the calculated band structure of β-Ag_2Te with SOC included (using experimental structure [24]). It is seen that the gap is around 80 meV, in good agreement with experimental data [1]. The present results can be also well compared to earlier calculations [25], except that those studies neglected the SOC and therefore got metallic state.

The β-Ag_2Te with distorted structure is now true insulating, but more importantly its topological nature is nontrivial due to the inverted band structure. Since the β phase has inversion symmetry, we can identify its topological nature by analyzing the parity of wave functions [9]. We have calculated the parities of occupied wave functions for time-reversal-invariant points in the BZ, it is confirmed that the product of parities of occupied bands is negative at the Γ point and positive for other points, which leads to a $Z_2 = 1$ topological insulator [9]. This topological nature should support gapless Dirac-type surface states. The calculated surface states for the plane perpendicular to the C axis are shown in the Fig. 4. It is clearly seen that we have single Dirac cone on the surface similar to Bi_2Te_3, and Bi_2Se_3 [15,19]. However, what is different is that the surface Dirac cone is highly anisotropic, and the Fermi velocity varies by about an order of magnitude moving around the cone. The broken rotational symmetry in this case is due to the absence of fourfold (in HgTe) or threefold (in Bi_2Se_3) rotational symmetry. The spin direction is locked with lattice momentum and the spin chiral texture shown in Fig. 4(b) corresponds to the chemical potential about 10 meV below the Dirac point. The spin direction of the surface states has out-of-plane component, which gives us more freedom to manipulate electron spin.

An effective $k \cdot p$ model can be established by considering only the preserved time-reversal symmetry for the surface state. The possible model Hamiltonian around Γ point is,

$$H(k) = A\sigma_x + B\sigma_y + C\sigma_z + DI_{2\times 2}. \quad (1)$$

where σ_x, σ_y, σ_z are Pauli matrix and $I_{2\times 2}$ is 2×2 identity matrix. $A(k_x, k_y)$, $B(k_x, k_y)$, $C(k_x, k_y)$, and $D(k_x, k_y)$ are functions of lattice momentum. Here it is noticed that we have defined the principal axis z to be along the C axis. In order to conserve the time-reversal symmetry, A, B, and C should contain only the odd terms of k_x and k_y, and D contains the even terms. We expand A and B up to the third order, D up to the second order, while include only the linear term for C because the out-of-plane component of spin is much smaller than the in-plane component,

$$A(\vec{k}) = c_1k_x + c_2k_y + c_3k_x^3 + c_4k_x^2k_y + c_5k_xk_y^2 + c_6k_y^3, \quad (2)$$

$$B(\vec{k}) = c_7k_x + c_8k_y + c_9k_x^3 + c_{10}k_x^2k_y + c_{11}k_xk_y^2 + c_{12}k_y^3, \quad (3)$$

$$C(\vec{k}) = c_{13}k_x + c_{14}k_y, \quad (4)$$

$$D(\vec{k}) = c_{15}k_x^2 + c_{16}k_y^2 + c_{17}k_xk_y. \quad (5)$$

The parameters can be obtained by fitting the surface states calculated from *ab initio* simulations. Both the shape and spin orientation of surface states can be well reproduced with the parameters listed in Ref. [26].

The existence of gapless Dirac surface states in β-Ag_2Te suggests that the unusual MR may have large contribution coming from the surface or interface. This scenario is supported by the fact that experimental samples, doped with excess Ag, are granular materials [3,27], which makes the interface contribution significant. Using the calculated Fermi velocity (3×10^7 cm/s in average) of Dirac surface states to evaluate Landau level spacing, we estimated that the quantum limit can be reached by only 10 Oe field under 5 K, or by 1.4 T field under 300 K, in agreement with experiment [3]. In the extreme case, if we assume that experimental carrier density (about 10^{17} cm^{-3} [3]) all goes into the interface region (assuming granular size about 60 nm), this will give a 2D density around 10^{11} cm^{-2}, which is still reasonably low (corresponding to Fermi level about 2 meV above Dirac point) and will occupy only the lowest Landau level of Dirac surface states under 1 T field. In reality, this density could be much lower due to inhomogeneity as has been addressed [4]. Once the quantum limit is reached, the linear MR behavior will be expected, while its absolute magnitude depends on other details of samples. On the other hand, the highly anisotropic surface states may cause large fluctuation of mobility, which may also help to explain the unusual MR behavior [27]. We have done similar calculations for Ag_2Se, and found that it is also topologically nontrivial with inverted band structure, while its β phase crystal structure is different from Ag_2Te.

In summary, we have shown by first principles calculations that β-Ag_2Te is a new binary topological insulator provided by nature, with highly anisotropic single surface Dirac cone. We suggest that the observed unusual MR behavior can be understood from its topological nature. We acknowledge the supports from NSF of China and that from the 973 program of China (No. 2007CB925000).

*hmweng@iphy.ac.cn
†daix@iphy.ac.cn
‡zfang@iphy.ac.cn

[1] R. Dalven, Phys. Rev. Lett. **16**, 311 (1966); R. Dalven and R. Gill, Phys. Rev. **159**, 645 (1967); P. Junod *et al.*, Philos. Mag. **36**, 941 (1977).
[2] S. A. Aliev and F. F. Aliev, Izv. Akad. Nauk SSSR, Neorg. Mater. **21**, 1869 (1985).
[3] R. Xu, A. Hussman, T. F. Rosenbaum, M.-L. Saboungi, J. E. Enderby, and P. B. Littlewood, Nature (London) **390**, 57 (1997).
[4] A. A. Abrikosov, Phys. Rev. B **58**, 2788 (1998); A. A. Abrikosov, Phys. Rev. B **60**, 4231 (1999).
[5] C. L. Kane and E. J. Mele, Phys. Rev. Lett. **95**, 146802 (2005).
[6] B. A. Bernevig and S. C. Zhang, Phys. Rev. Lett. **96**, 106802 (2006).
[7] J. E. Moore and L. Balents, Phys. Rev. B **75**, 121306 (2007).
[8] L. Fu, C. L. Kane, and E. J. Mele, Phys. Rev. Lett. **98**, 106803 (2007).
[9] L. Fu and C. L. Kane, Phys. Rev. B **76**, 045302 (2007).
[10] L. Fu and C. L. Kane, Phys. Rev. Lett. **100**, 096407 (2008); X.-L. Qi *et al.*, Phys. Rev. Lett. **102**, 187001 (2009).
[11] X.-L. Qi, T. L. Hughes, and S. C. Zhang, Phys. Rev. B **78**, 195424 (2008); A. M. Essin, J. E. Moore, and D. Vanderbilt, Phys. Rev. Lett. **102**, 146805 (2009).
[12] X. L. Qi, Y. S. Wu, and S. C. Zhang, Phys. Rev. B **74**, 085308 (2006); F. D. M. Haldane, Phys. Rev. Lett. **61**, 2015 (1988); M. Onoda and N. Nagaosa, Phys. Rev. Lett. **90**, 206601 (2003); R. Yu *et al.*, Science **329**, 61 (2010).
[13] B. A. Bernevig *et al.*, Science **314**, 1757 (2006); M. König *et al.*, Science **318**, 766 (2007); X. Dai *et al.*, Phys. Rev. B **77**, 125319 (2008).
[14] D. Hsieh *et al.*, Nature (London) **452**, 970 (2008); J. C. Y. Teo, L. Fu, and C. L. Kane, Phys. Rev. B **78**, 045426 (2008); H.-J. Zhang *et al.*, Phys. Rev. B **80**, 085307 (2009).
[15] H. J. Zhang *et al.*, Nature Phys. **5**, 438 (2009); Y. Xia *et al.*, Nature Phys. **5**, 398 (2009); Y. L. Chen *et al.*, Science **325**, 178 (2009).
[16] B. Yan *et al.*, Europhys. Lett. **90**, 37002 (2010); T. Sato *et al.*, Phys. Rev. Lett. **105**, 136802 (2010).
[17] H. Lin *et al.*, Nature Mater. **9**, 546 (2010); S. Chadov *et al.*, Nature Mater. **9**, 541 (2010); D. Xiao *et al.*, Phys. Rev. Lett. **105**, 096404 (2010).
[18] W. Feng *et al.*, Phys. Rev. Lett. **106**, 016402 (2011).
[19] W. Zhang *et al.*, New J. Phys. **12**, 065013 (2010).
[20] In general, to get the gapless surface states (preventing the coupling between top and bottom surfaces), a thick enough slab is necessary, which is out of the reach of present *ab initio* techniques. Using the Wannier functions, a effective model can be constructed for a thick enough slab (while neglecting surface relaxations), from which the gapless surface states can be calculated. Such a procedure has been successfully applied to Bi_2Se_3 family compounds [19].
[21] H. Kikuchi *et al.*, J. Phys. Condens. Matter **9**, 6031 (1997).
[22] C. Y. Moon and S. H. Wei, Phys. Rev. B **74**, 045205 (2006); A. Fleszar and W. Hanke, Phys. Rev. B **71**, 045207 (2005).
[23] J. Heyd *et al.*, J. Chem. Phys. **124**, 219906 (2006).
[24] A. van der Lee and J. L. de Boer, Acta Crystallogr. Sect. C **49**, 1444 (1993).
[25] S. Kashida *et al.*, Solid State Ionics **148**, 193 (2002); C. M. Fang *et al.*, J. Phys. Chem. Solids **63**, 457 (2002).
[26] The fitted parameters (with energy unit in eV and length unit in Å) are: $c_1 = -1.192$, $c_2 = 0.781$, $c_3 = -14.935$, $c_4 = 17.443$, $c_5 = 9.963$, $c_6 = 11.609$, $c_7 = -1.807$, $c_8 = 0.822$, $c_9 = -12.415$, $c_{10} = 13.148$, $c_{11} = -55.148$, $c_{12} = 19.788$, $c_{13} = -0.217$, $c_{14} = 0.116$, $c_{15} = -1.559$, $c_{16} = 2.687$, $c_{17} = -9.705$.
[27] M. M. Parish and P. B. Littlewood, Nature (London) **426**, 162 (2003).